FINAL REPORT

Assessing the Potential Consequences of Subsurface Bioremediation: Fe-oxide Bioreductive Processes and the Propensity for Contaminant-colloid Co-transport and Media Structural Breakdown

SERDP Project ER-2130

MAY 2017

Dr. Mark Radosevich
University of Tennessee

SERDP
DOD ▪ EPA ▪ DOE

Page Intentionally Left Blank

Page Intentionally Left Blank

REPORT DOCUMENTATION PAGE

Form Approved
OMB No. 0704-0188

1. REPORT DATE *(DD-MM-YYYY)*	**2. REPORT TYPE**	**3. DATES COVERED** *(From - To)*
12-05-2017	Final	07/07/2015 – 12/31/2016

4. TITLE AND SUBTITLE

Assessing the potential consequences of subsurface Bioremediation: Fe-oxide bioreductive processes and propensity For contaminant-colloid

5a. CONTRACT NUMBER
W912HQ-11-C-0067

5b. GRANT NUMBER

5c. PROGRAM ELEMENT NUMBER

6. AUTHOR(S)
Mark Radosevich
Jie Zhaung
Sean Schaeffer

5d. PROJECT NUMBER
ER-2130

5e. TASK NUMBER

5f. WORK UNIT NUMBER

7. PERFORMING ORGANIZATION NAME(S) AND ADDRESS(ES)

The University of Tennessee
2621 Morgan Circle drive, 225
Morgan Hall
Knoxville, TN 37996-4514

8. PERFORMING ORGANIZATION REPORT NUMBER

9. SPONSORING / MONITORING AGENCY NAME(S) AND ADDRESS(ES)
USAED (HQUSACE)
C/O USACE Finance Center
5722 Integrity Drive
Millington, TN 38054-5005

10. SPONSOR/MONITOR'S ACRONYM(S)
SERDP

11. SPONSOR/MONITOR'S REPORT NUMBER(S)

12. DISTRIBUTION / AVAILABILITY STATEMENT
Approved for Public release; distribution is unlimited

13. SUPPLEMENTARY NOTES

14. ABSTRACT

Bioremediation is an attractive approach for decontamination and/or immobilization of organic and inorganic groundwater contaminants based on low cost and effectiveness. The approach typically involves manipulation of the physical and chemical environment to achieve conditions that will stimulate the desired biotic and/or abiotic processes necessary to degrade or immobilize the contaminants in situ. However, even though contaminant biotransformation may be achieved, altering the chemical environment may be altered and promote unintended processes that may accelerate or retard subsequent fate and transport of residual contaminants or degrade groundwater quality. For example, many subsurface bioremediation approaches involve the introduction of carbon substrates such as acetate or lactate (i.e. electron donors) that stimulate anaerobic respiration whereby solid phase mineral oxides of Fe and Mn serve as electron acceptors. During this process oxidized forms of iron are reduced to Fe(II) solubilizing the iron oxide. Secondary precipitation of iron can then result in the formation of colloidal iron minerals. Adsorption of residual contaminants to these colloids may enhance contaminant transport via colloid-facilitated transport. Additionally, if microbial biomass production and colloid generation are significant enough pore clogging may occur; reducing the hydraulic conductivity of the porous media. Thus altering the indigenous properties of the subsurface media can significantly impact coupled processes controlling contaminant bioremediation (e.g. secondary mineral precipitates, permeability, and changes in microbial activity).

15. SUBJECT TERMS

bioremediation, groundwater

16. SECURITY CLASSIFICATION OF:			**17. LIMITATION OF ABSTRACT**	**18. NUMBER OF PAGES**	**19a. NAME OF RESPONSIBLE PERSO**
a. REPORT	**b. ABSTRACT**	**c. THIS PAGE**		37	Mark Radosevich
					19b. TELEPHONE NUMBER *(include are code)* 865-974-7454

Page Intentionally Left Blank

Preface

Dr. Phillip Jardine, the original PI of the project passed away in July, 2014 with approximately one year remaining on the original project duration. The project was suspended for more than a year before a new team was identified and a revised plan of remaining work was approved by SERDP. During that period the PI leading the modeling effort of the original proposed work retired and all submitted charges from the Harvard University sub-contract were resolved and the sub-contract was suspended. Based on careful examination of previously submitted progress reports, publications and other recoverable information the new team concluded the proposed activities of Task A and C were partially or nearly complete but the progress toward Task B was minimal. Further in his final IPR Dr. Jardine identified methodological barriers in the experimental design of Task B and questioned if the goals were achievable with the time and funding remaining. In an effort to remain as true to the original proposal as possible the new project team decided to focus the remaining effort and resources on Task B, in spite of Dr. Jardine's concerns, since it was the objective with the least progress and further work on tasks A and C would require analytical capabilities and resources that were unavailable to the new project team. A new model experimental system using water-stable soil aggregates was developed to preserve an element of soil structure while allowing continued experimentation of Task B objectives at the laboratory column scale. This final report therefore focuses on Task B and the progress made under the revised project plan initiated July 1, 2015.

Abstract

Bioremediation is an attractive approach for decontamination and/or immobilization of organic and inorganic groundwater contaminants based on low cost and effectiveness. The approach typically involves manipulation of the physical and chemical environment to achieve conditions that will stimulate the desired biotic and/or abiotic processes necessary to degrade or immobilize the contaminants *in situ*. However, even though contaminant biotransformation may be achieved, altering the chemical environment may be altered and promote unintended processes that may accelerate or retard subsequent fate and transport of residual contaminants or degrade groundwater quality. For example, many subsurface bioremediation approaches involve the introduction of carbon substrates such as acetate or lactate (i.e. electron donors) that stimulate anaerobic respiration whereby solid phase mineral oxides of Fe and Mn serve as electron acceptors (Fig. 1). During this process oxidized forms of iron are reduced to Fe(II) solubilizing the iron oxide. Secondary precipitation of iron can then result in the formation of colloidal iron minerals. Adsorption of residual contaminants to these colloids may enhance contaminant transport via colloid-facilitated transport. Additionally, if microbial biomass production and colloid generation are significant enough pore clogging may occur; reducing the hydraulic conductivity of the porous media. Thus *altering the indigenous properties of the subsurface media* can significantly impact coupled processes controlling contaminant bioremediation (e.g. secondary mineral precipitates, permeability, and changes in microbial activity).

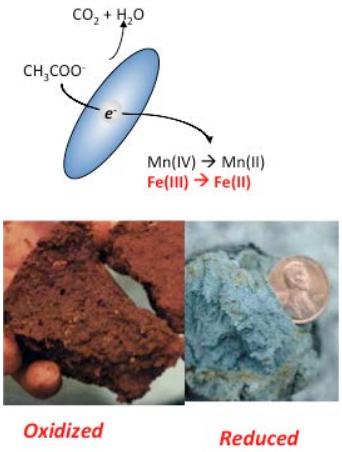

Fig.1. Anaerobic respiration by Fe(III)-reducing bacteria using acetate as an electron donor resulting in the reduction of Fe(III) to Fe(II).

The overall goal of the research program was to provide new fundamental data and numerical simulations to assess the impact of bioreductive remedial processes on rates and mechanisms of colloid generation and the subsequent impact on contaminant co-transport, as well as the propensity for irreversible changes in soil structure following bioremediation. The objectives were resolved by a technical approach that included three well-integrated experimental tasks follows:

Task A: Quantify the *impact of time-dependent bioreduction reactions* on (a) the formation of secondary iron-oxide mineral precipitates for different Fe(III)-oxide minerals, and (b) the changes in microbial community structure and activity during the reduction process, which in-turn will dictate contaminant destruction.

Task B: Investigate *media structural breakdown* and mineral dispersion during bioremediation.

Task C: *Development of a modeling tool* of coupled hydrological, geochemical, and microbial processes controlling Fe(III)-oxide bioreduction and the impact of spatially variable secondary mineral precipitates (Task A) and permeability (Tasks A and B).

Results include the following:

Tasks A and C were largely addressed by the previous research team and summarized to the best of our ability as follows:

- The research quantified coupled hydrological, geochemical, microbial, and mineralogical processes to assess the importance of Fe(III)-oxide reduction on contaminant destruction.
- These experiments showed that the dominant terminal electron accepting process (metal versus sulfate reduction) varied as a function of iron oxide type and crystallinity and solution chemistry.
- Significant secondary mineral formation occurred in all columns with primarily magnetite formed in the ferrihydrite columns and sulfur- and sulfide-bearing phases dominating goethite and hematite amended columns. Microbial community analyses were consistent with the secondary minerals formed. Namely, when highly crystalline Fe-oxides were the dominant mineral phase prior to bioreduction, Fe-reduction rates were slow; allowing sulfate reduction to out compete iron reduction resulting in communities largely dominated by sulfate-reducing bacteria.
- Small porosity changes were evident in all the columns and substantial colloidal transport was observed in the ferrihydrite columns only.
- Bioreduction under these conditions may therefore lead to iron oxides serving as a contaminant (e.g. As) vector in subsurface sediments.
- Predictive models were successfully developed from the initial column experiments as described above in Tasks A and C.
- The results from tasks A and C culminated in the following publication:
  C.M. Hansel, C.L. Lentini, Y. Tang, D.T. Johnston, S.D. Wankel, and P.M. Jardine. 2015. *Dominance of Sulfur-fueled Iron Oxide Reduction in Low Sulfate Freshwater Sediments.* ISME Journal 9, 2400-2412.

Task B (largely addressed by the substitute project team):

- Experiments intended to investigate media structural breakdown with undisturbed subsurface media were unsuccessful and deemed intractable at the experimental scale investigated (See Jardine IPR May 2014).
- Thus, tracer transport studies before and after Fe(III)-bioreduction were executed in re-packed column experiments using water-stable soil aggregates to examine potential changes in pore-structure and hydraulic conductivity. The results showed that Fe(III) bioreduction resulted in aggregate breakdown and colloid dispersion depending on the extent of Fe(III) reduction and altered the pore structure and chemical reactivity of the porous media. However, under the experimental conditions, only minor changes in tracer transport were observed suggesting that medium structural breakdown poses a negligible threat to groundwater quality. However, it should be noted that the experimental design did not allow for assessment of the potential for down-gradient changes in the redox environment that may lead to precipitation of secondary mineral phases and clay colloids with potential pore-clogging and decreases in hydraulic conductivity.

Objectives

The original proposal aimed to address FY 2011 Statement of Need ERSON-11-03 entitled "Improved Understanding of Impacts to Groundwater Quality Post-Remediation". As stated in the original proposal "The overall goal was to provide new fundamental data and numerical simulation on the impact of bioreductive remedial processes on rates and mechanisms of colloid generation and their impacts on contaminant co-transport, as well as the propensity for irreversible changes in soil structure following bioremediation." The specific objectives of the original proposal were:

1. Develop an improved understanding and predictive capability of the impacts of subsurface bioremediation on the kinetics and mechanisms of (a) media structural breakdown and loss in permeability as the result of aggregate dispersion and (b) the generation of Fe- and clay-rich colloids and secondary mineral precipitates.
2. Quantify the fate and transport of colloid particles in heterogeneous subsurface media as a function of changing hydrological, geochemical, and microbiological processes, and investigate the impacts of accelerated contaminant co-transport vs. medium pore clogging on post-bioremediation groundwater quality.
3. Develop predictive models to establish bioremediation protocols and groundwater monitoring strategies that optimize contaminant destruction and immobilization while minimizing the disruption of the subsurface media structure and the formation of mobile colloids.

Background

During subsurface bioremediation brought about by electron donor addition anaerobic conditions are created leading to the stimulation of iron reducing and/or sulfate reducing bacteria (Chapelle and Lovley, 1992; Methe et al., 2003). Subsequently oxidized forms of iron are reduced to Fe(II) solubilizing the iron oxide minerals. The soluble Fe(II) and secondary precipitation of iron can result in abiotic transformation of contaminants and/or result in the release of colloidal clay and iron mineral colloids (Pedersen et al., 2006; Thompson et al., 2006). Adsorption of residual contaminants to these colloids may enhance contaminant transport via colloid-facilitated transport (Bose and Sharma, 2002; Zhuang et al., 2003). Additionally, if biomass production and colloid production are significant enough pore clogging may occur and potentially reducing hydraulic conductivity of the porous media down gradient from the contaminated zone. Alternatively advective flow paths and increased hydraulic conductivity may potentially result with significant aggregate breakdown. Thus *altering the indigenous properties of the subsurface media* can significantly impact coupled processes controlling contaminant fate and transport and have unintended secondary impacts on the properties of the porous media and potentially groundwater quality (e.g. secondary mineral precipitates, permeability, changes in microbial activity).

Transport of solutes and colloids in soil is influenced by physical and chemical properties, solution chemistry, and hydrological conditions (Zhuang et al., 2004; 2005; 2007). Much research has been conducted to examine the transport of various solutes and colloids at varying scales from laboratory columns (repacked or undisturbed) to field scale (Vilks et al., 1997; McKay et al., 2000). Flow pathways and soil surface chemistry have been demonstrated to

control the transport of solutes and colloids (Bradford and Torkzaban, 2008). Chemical and biological processes, such as those involved in bioremediation, may cause alteration of flow paths and mineral interfacial properties. However, the potential impacts of bioremediation engineering on changes in media pore structure and mineral surface chemistry that may potentially impact the transport of solutes and colloids are not well understood.

Anaerobic bioremediation is one of the most attractive technologies for subsurface soil and water remediation based on cost and effectiveness (Ellis et al., 2000; Coates and Anderson, 2000). Anaerobic bioremediation generally aims to create anaerobic conditions via addition of soluble electron donors such as acetate and lactate or more complex substrates, for stimulating microorganisms that degrade organic contaminants (e.g. chlorinated hydrocarbons) and reduce heavy metals and radionuclides to insoluble forms thereby immobilizing them *in situ* (Aulenta et al., 2006). Once anaerobic conditions are achieved anaerobic respiration with alternate electron acceptors is stimulated leading to biologically-mediated reduction of Fe(III)-oxide minerals (the most common mineral oxide of many subsurface environments) and the formation of soluble Fe(II) (Caldwell et al., 1999; Weber et al., 2006). The indigenous Fe-oxide minerals serve a very important role as aggregating agents that "cement" clay particles together into aggregates (Goldberg and Glaubig, 1987; Goldberg et al., 1990). Reduction of Fe(III)-oxide under anaerobic conditions may cause disintegration of soil aggregates and generate colloids (Hansel et al., 2005; De-Campos et al., 2009). These processes may cause pore structure disruption, altering pore connectivity, flow paths, and permeability. The transport of solutes and colloids could either be promoted or inhibited by these alterations. The formation and mobilization of colloids can also act as possible vectors to facilitate co-transport of solutes and toxic metals in soil and groundwater (McCarthy and McKay 2004; Kuhnen et al., 2000; Hassellöv and von der Kammer, 2008; Maurice and Hocella, 2008). The reduction of Fe(III)-oxide may also change the surface properties of soil, influencing the transport processes (Hansel et al., 2003; Jardine, 2008).

The objective of this work was to assess the influence of biologically-mediated Fe(III)-oxide reduction on pore-structure and permeability of well aggregated model soil columns. Alterations of pore-structure were investigated by conducting tracer breakthrough tests with three different diffusible and non-diffusible tracers both before and after periods of stimulated Fe(III)-bioreduction by introducing acetate as an electron donor. The three different types of tracers were bromide, 2,6-difluorobenzoic acid (DFBA), and silica-shelled silver nanoparticles (SSSNP). The results showed that while some changes in pore structure and mineral surface reactivity were evident after Fe(III)-bioreduction, the impact on overall transport of the tracers was negligible.

Materials and Methods

2.1 Porous Media

2.1.1 Sand and Goethite-Coated Sand

Ottawa quartz sand (300~355 μm) and goethite coated Ottawa quartz sand of the same sizes were used to evaluate the transport of silica-shelled silver nanoparticles (SSSNP) and the effect of porous medium surface chemistry on SSSNP transport. The original proposal intended to use bacteriophage (MS-2) as non-diffusing particle tracers. After careful consideration and based on our past experience, use of phage for the purposes of this study would be analytically difficult and experimentally problematic. Therefore the SSSNP nanoparticles of similar size to MS-2 and similar surface properties to silicate-dominated porous media were used in place of

phage. Prior to packing the columns, the sand was chemically cleaned to remove metal oxides using the method as described in Zhuang et al. (2009). A portion of clean sand was then used to prepare goethite-coated sand following the method as described in Zhuang and Jin (2008).

2.1.2 Water-Stable Soil Aggregates

We were unable to collect undisturbed sub-surface porous media suitable for the column-scale experiments that were conducted in an anaerobic chamber. Therefore to maintain a strong initial element of pore structure in disturbed repacked columns we elected to conduct model experiments in columns packed with water-stable soil aggregates. Iron oxide-rich soil samples were collected from an eroded agricultural site mapped as the Decatur silty clay loam. The Decatur series is a fine, kaolinitic, thermic rhodic Paleudults. Evidence of significant erosion was present at the collection site and particle size analysis revealed the collected material fell within the "clay" textural class. The citrate-bicarbonate-dithionite extractable iron (Mehra and Jackson, 1960) of this soil was 5.5% as measured by the ferrozine method (Viollier et al. 2000). Soil aggregates were extracted by wet sieving soils through 2000, 250, and 53 μm sieves using the modified method as described in Zhuang et al., (2008). Two fractions of water-stable soil aggregates, macroaggregates (250~2000 μm) and microaggregates (53~250 μm) were collected and then air-dried for experimental use. The extractable iron of macroaggregates and microaggregates were 5.2% and 4.7%, respectively.

2.2 Transport Experiments

2.2.1 Multiple Tracers

Three tracers were used for transport experiments, including bromide (ionic tracer), 2,6-difluoro-benzoic acid (2,6-DFBA) (molecular tracer with lower diffusivity than Br^-) (Mayes et al., 2003), and SSSNP (particle tracer) (Fig. 2). The SSSNP was purchased from nanoComposix (http://nanocomposix.com/) and has a core of silver nanoparticles with average diameter of 106 nm. The silver cores are encased in a shell of silica with average thickness of 22 nm, resulting in a total particle diameter of 150 nm. The SSSNP was slightly negatively charged, with measured zeta potential of -5.7 mV at pH 8. SSSNP was specifically selected as a "non-diffusing" tracer and potentially as a non-reactive tracer given the silica shell surrounding the silver-core (http://nanocomposix.com/). Given the particle size, transport of these particles should be restricted to advective flow paths only. To our knowledge these particles have not previously been used as tracers for transport studies. One advantage to using these particles instead of other previously used particle tracers such as viruses was their resistance to biotic and abiotic breakdown and the ease and accuracy of quantification in the effluent samples using graphite furnace atomic absorption spectroscopy and the convenience to distinguish introduced colloids (SSSNP) from native soil colloids for mechanistic understanding of transport processes.

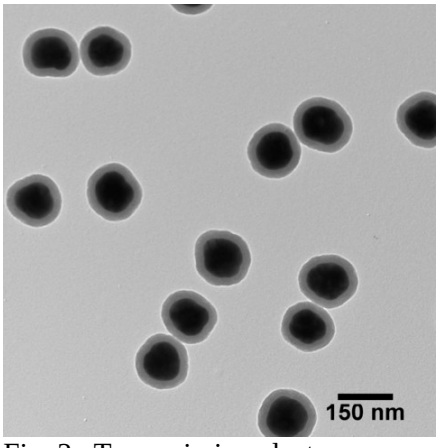

Fig. 2. Transmission electron micrograph of silica-coated silver nanoparticles used as non-diffusing particle tracers in this study. Image taken from NanoComposix website (http://nanocomposix.com/

2.2.2 Column Transport Experiments

Three separate experiments were conducted. The first were conducted in columns packed with sand or goethite-coated sand to evaluate the use of SSSNP as particle tracers (Experiment type I). The second experiment (Experiment type II) was conducted with inoculated soil aggregates under anaerobic conditions and had two objectives i) to establish the best method to pack and inoculate the soil aggregate columns and ii) to collect tracer breakthrough data before and after Fe(III)-bioreduction and to test pressure transducers connected at ports along the length of the columns. At the time Experiment type II was executed only two columns were available for use. Thus, one column was used for wet and dry packed soil aggregates, respectively. During the wet packing, evidence of dramatic aggregate dispersion was observed and once flow was initiated the packing cracked and was deemed no longer useable for transport experiments (Fig. 4). Thus the Experiment type II includes data collected from the single remaining column. In the third experiment (Experiment type III) additional columns were constructed so that the type II experiment could be repeated with control and replicated columns. In addition, the Fe(III)-bioreduction phase was extended from 20 d to 60 d in the type III experiment.

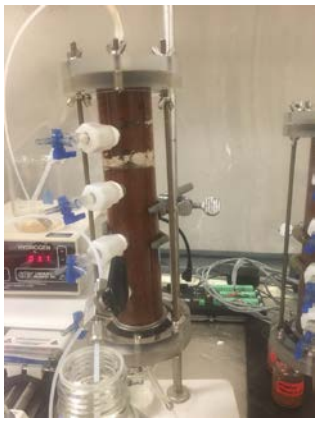

Fig. 4. Wet packed soil column showing severe cracking of packing material upon initiation of flow.

All transport experiments were conducted in plexiglass (acrylic) columns, 25 cm in length and 3.8 cm in inside diameter (Fig. 5). The columns were fitted with ports connected to pressure sensors (Honeywell Sensing and Control, Inc.) separated by 5 cm intervals along the flow path and at the effluent end of the columns. Real-time hydrostatic pressure data was collected with CR1000 Measurement and Control Systems data loggers (Campbell Scientific, Inc., Logan Utah). The difference in pressure along the flow path was then used to calculate hydraulic conductivity in different sections of the columns. The saturated transport experiments were conducted in a very similar manner as described by (Wang et al. 2013). The general experimental design for soil columns included sequential tracer experiments conducted both before (i.e. phase 1) and following (i.e. phase 3) a period of stimulated Fe(III)-bioreduction (i.e. phase 2) achieved through the introduction of acetate in the input solution. The sand columns were wet packed with the clean sand or goethite-coated sand, while the soil aggregates were dry packed. The soil aggregate packed columns were flushed with carbon dioxide to replace the air in the pores within the soil aggregate matrix. Then, the columns were flushed with KCl solution (0.67 mM, pH 6.5) to dissolve the carbon dioxide into the solution for

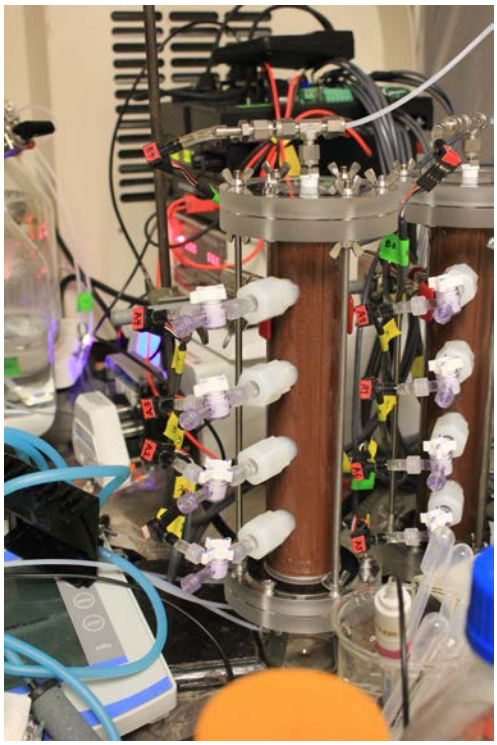

Fig. 5. Photograph of an experimental column used to conduct tracer tests before and after Fe(III) bioreduction.

complete saturation of the entire column. The saturated columns were then used for performing the tracer transport experiments as described by Wang et al. (2013). The effluent was collected by Retriever II fraction collectors for analysis of bromide, 2,6-DFBA, SSSNP, Fe(II), and colloids as described in Section 2.4. See Appendix 1 for more specific details regarding the set-up, packing and execution of column experiments.

2.3 Stimulated Bioreduction Experiments

2.3.1 Iron Reducing Bacteria

To ensure a significant rate of Fe(III) bioreduction, the soil aggregates were inoculated with laboratory grown culture of *Geobacter sulfurreducens* (Caccavo et al., 1994) prior to packing the columns. The *Geobacter* was cultured in DCB-1 medium at 30 °C as described by Löffler and his coworkers (Yan et al., 2012). Once the cultures reached stationary phase (3-5 d), 200 mL of the culture was centrifuged at 5,000 rpm. The bacterial pellet was then resuspended in 10 mL growth medium for inoculation of air-dried water-stable soil aggregates.

Inoculation and packing of the soil aggregate columns was performed under anaerobic conditions inside an anaerobic chamber with an atmosphere of 80/20 N_2/CO_2. Soil aggregates were inoculated with *Geobacter sulfureducens* by spraying a minimal volume of the prepared cell suspension onto the soil aggregates that were thinly spread on a tray. The soil aggregates were continuously mixed during this process to achieve uniform distribution of bacteria. Inoculated soil aggregates were then packed into the columns as described above. The packed columns were flushed with carbon dioxide, followed by flushing with artificial groundwater (AGW) to achieve fully saturated conditions. The AGW had a total ionic strength of 2 mM and a pH value of 7.5, consisting of $CaCl_2$ (0.075 mM), $MgCl_2$ (0.082 mM), KCl (0.051 mM), and $NaHCO_3$ (1.5 mM).

A tracer transport experiment for soil columns (experimental phase 1) was conducted to assess the transport of tracers before any acetate addition and Fe(III)-bioreduction. Following the completion of phase 1 tracer test, acetate-treated columns received AGW solution with acetate, trace elements, and vitamins. The control column received only AGW solution (experiment phase 2). Please note in the subsequent soil columns of experiment type III, the vitamins and other trace elements were excluded from the AGW input solution but the total ionic strength was equivalent to experiment type II. Acetate added to the treatment columns served as the electron donor for *Geobacter*. Trace elements and vitamins were supplied to ensure healthy growth of *Geobacter* in the first soil column experiment (Experiment type II) but were excluded in subsequent soil column experiment (Experiment type III). During phase 2, the Fe(III)-bioreduction phases were conducted for different lengths of time, 20 days for short-term experiment (Experiment type II) and 59 days for long-term experiment (Experiment type III). During phase 2 (acetate addition), effluent samples were analyzed for the concentrations of Fe(II), Fe(III) and colloids as described in Section 2.4. The columns were flushed briefly with AGW before starting another tracer transport experiment (phase 3).

2.4 Analytical Methods

Bromide concentration was in the effluent fractions was determined either by using a bromide-selective electrode (Thermo Scientific Orion bromide electrode Ionplus® Sure-Flow®) or by ion chromatography. The concentration of 2,6-DFBA was measured by a modified HPLC method as described by (Kubica et al., 2015). Briefly, 2,6-DFBA was resolved from other effluent constituents using an Econosphere C-18 RP column (5 μm, 150 mm x 4.6 mm) with

isocratic elution using a mobile phase consisting of 95% K-phosphate buffer (5 mM; pH 3) and 5% acetonitrile (V/V) at a flow rate of 1.0 ml min^{-1}. 2,6-DFBA was quantified using UV absorption at 200 nm and the concentration was calculated via linear regression of peak area of external 2,6-DFBA standard solutions. Significant sample matrix effects on the elution of 2,6-DFBA were observed thus it was critical that the sample matrix match the elution buffer as closely as possible to achieve accurate quantification. This was achieved by diluting the samples in mobile phase 1:10 (V/V) prior to analysis. All samples were filtered through 0.1 μm filters prior to analysis.

The concentration of SSSNP was determined as the concentration of silver by graphite furnace atomic absorption spectrometry using a Perkin-Elmer Graphite Furnance AA. The concentrations of Fe(II) and Fe(III) in the effluent were measured using a modified Ferrozine method (Stookey, 1970). Colloid concentration was determined by centrifuging the effluent sample and measuring the mass of pellets after oven-drying.

2.5 Numerical Modeling

The HYDRUS-1D (Simunek et al., 2008) codes were used to simulate the transport of bromide, 2,6-DFBA, and SSSNP. The HYDRUS code simulates saturated water flow using the Richards equation. Bromide and 2,6-DFBA transport were simulated using the advection-dispersion equation (ADE). SSSNP transport and retention was simulated using the ADE with first-order terms for kinetic retention and release.

2.6. Microbial Community Composition

At the conclusion of the long-term Fe(III)-bioreduction experiment the two acetate-treated and control columns were deconstructed by dividing them into five section along the flow path. Soil from each section was sampled and whole soil DNA was extracted using the MoBio Powersoil DNA extraction kit (Qiagen, Germantown, MD). The concentration of DNA was quantified using picogreen. The DNA was used to assess microbial community composition by sequencing and analysis of barcoded 16S rRNA gene libraries through Hudson Alpha Genomics (https://gsl.hudsonalpha.org/index) using the MiSeq Illumina sequencing platform and the resulting sequence data was analyzed using MUTHER software package (Kozich et al., 2013).

2.7. Iron and Colloid Concentration in Sectioned Columns

Soil samples from the sectioned columns were homogenized and 5-g of soil from each sample was placed in 50-ml centrifuge tubes. In each tube, 15-mL of phosphate buffer (1.44 g/L $Na_2HPO_4 \bullet 7H2O$, 0.24 g/L KH_2PO_4, pH 7.0) was then added and shaken horizontally in ice water bath for 30 min. All tubes were centrifuged in 4000 g. The supernatant solution was filtered through 0.22 μm filters and iron concentration was determined as described by Viollier et al. (2000). Before filtration, 5-ml of solution was collected and centrifuged at 12,000 g for colloid content determination.

Results and Discussion

3. Results and Discussion

3.1 Transport of Different Tracers

In Type I experiments, clean and goethite-coated quartz sands were used as the porous media to evaluate the use of SSSNP as non-diffusing particle tracers and bromide was also included to ensure there was no abnormalities with the columns themselves. As a conservative tracer, bromide showed complete and ideal transport behavior with or without goethite coating on the sand (Fig. 6). The mobility of SSSNP in the clean sand eventually reached a maximum relative concentration of 0.85, in spite of significant retardation. However, almost no SSSNP moved through the goethite-coated sand column, suggesting a strong attachment of SSSNP on the iron oxide surfaces. The fitted parameters of the breakthrough curves (BTCs) of SSSNP showed faster attachment and slower detachment of SSSNP in goethite-coated sand, than in the uncoated sand , and the maximum normalized solid phase concentration of SSSNP was 3-orders of magnitude higher in the goethite-coated sand suggesting a strong affinity of the SSSNP nanoparticles for the iron-oxide surface (Table 1).

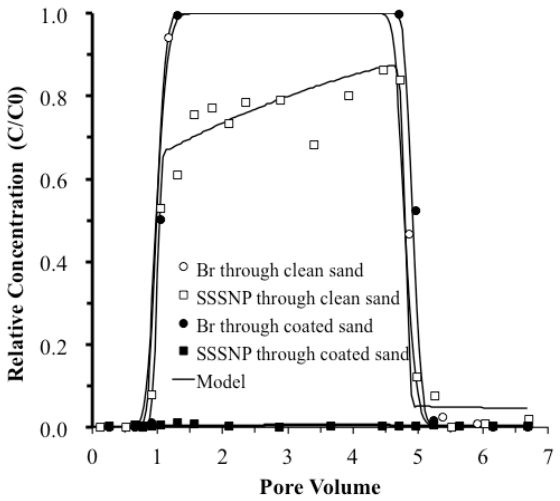

Fig. 6. Transport of bromide and SSSNP through clean sand and goethite coated sand.

Table 1. Model fitted parameters for SSSNP breakthrough curves in quartz sand and goethite-coated sand columns.

SSSNP	Sand Columns	
	Sand	Geothite-coated sand
S_{max}	0.56	12
Attachment Coefficient (min^{-1})	0.007	0.100
Detachment Coefficient (min^{-1})	0.001	0.0003

3.2 Fe(III)-Bioreduction and Tracer Transport: Short-term acetate injection

The breakthrough of bromide occurred at approximately one pore volume before and after the Fe(III)-bioreduction (Fig. 7), indicating that Fe(III) bioreduction did not affect the transport of this conservative tracer. Transport of 2,6-DFBA exhibited some retardation and tailing in the tracer breakthrough experiment before Fe(III) bioreduction (Fig. 7 and 8). In comparison, after Fe(III)-bioreduction treatment the retardation and tailing of 2,6-DFBA transport was eliminated suggesting that either physical and/or chemical changes during the Fe(III)-bioreduction occurred which enhanced the transport of 2,6-DFBA (Figs. 7 and 8). SSSNP exhibited a very pronounced response to the Fe(III)-bioreduction treatment, inconsistent with its transport behavior in clean and goethite-coated sand. Almost no breakthrough of SSSNP was observed before Fe(III)-bioreduction, whereas the relative SSSNP concentrations in effluent reached 0.3 after the Fe(III)-bioreduction (Fig. 7) . The detection of soluble Fe(II) in the effluent indicated reduction of soil Fe(III) by *Geobacter* and/or other iron-reducing bacteria (Fig. 9). The increase in effluent Fe(II) concentrations in the first two weeks corresponded to the increase in microbial activity as acetate was added to the input solution (Fig. 9). The effluent Fe(II) concentrations plateaued after 20 days of acetate injection, suggesting termination of Fe(III) bioreduction (Fig. 9). The accumulated amount of Fe(II) in the effluent was approximately 7 mg or about 0.04% of the total iron in the column. No Fe(III) oxides or other colloids were detected in the effluent during the experiment. Although only a very small fraction of total Fe(III) was reduced to soluble Fe(II) (assuming there was no secondary precipitation of Fe in the column), the influence Fe(III) reduction on the transport of 2,6-DFBA and SSSNP was significant. We attribute this effect to the reduction of the most bioavailable Fe(III) on the external surfaces of the soil aggregates, especially the Fe(III) existing along the advective pathways that are most accessible by microorganisms and tracers. Removal of surface iron oxides during bioreduction could reduce positive electrical charges and roughness on mineral surfaces, leading to an increase in tracer transport. Further research is needed to verify this hypothesis.

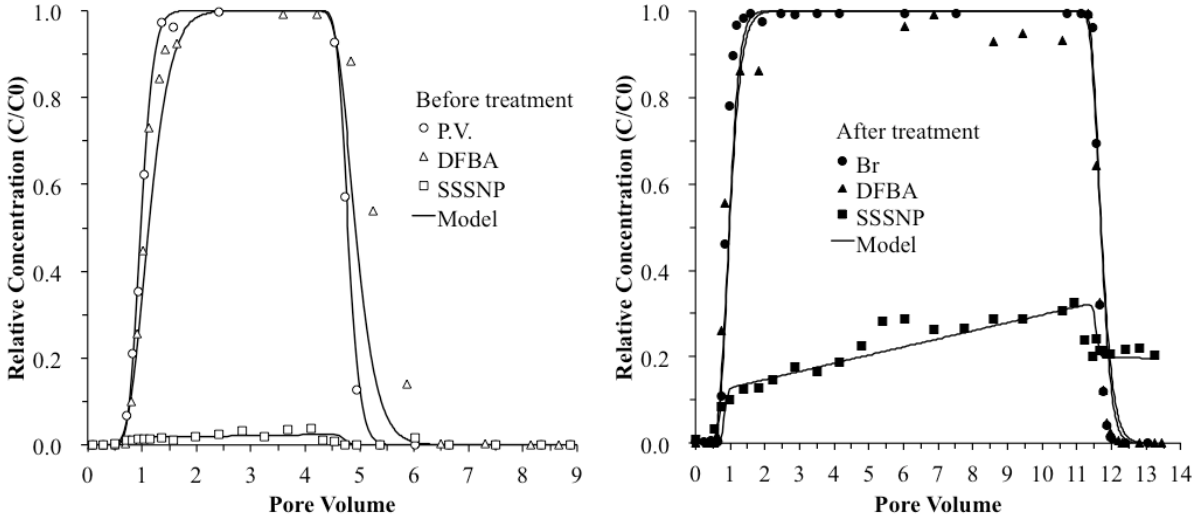

Fig. 7. Tracer breakthrough curves in columns packed with water stable soil aggregates before (Left) and after (right) Fe(III)-bioreduction for 20 d.

The parameters of model fitted BTCs of 2,6-DFBA and SSSNP in transport experiments for the short-term and long-term Fe(III)-bioreductions experiments are summarized in Table 2. The estimated dispersivity of 2,6-DFBA during transport was similar before and after the Fe(III)-bioreduction phase while the estimated 2,6-DFBA sorption coefficient was about one order of magnitude lower after Fe(III)-bioreduction (Table 2). The most notable impact on tracer transport was for SSSNP. The estimated maximum solid phase concentration in the post-treatment tracer test was one fourth that of the pre-treatment tracer test with a lower attachment coefficient. The estimated detachment coefficient was 100-fold greater in the post-treatment tracer test (Table 2).

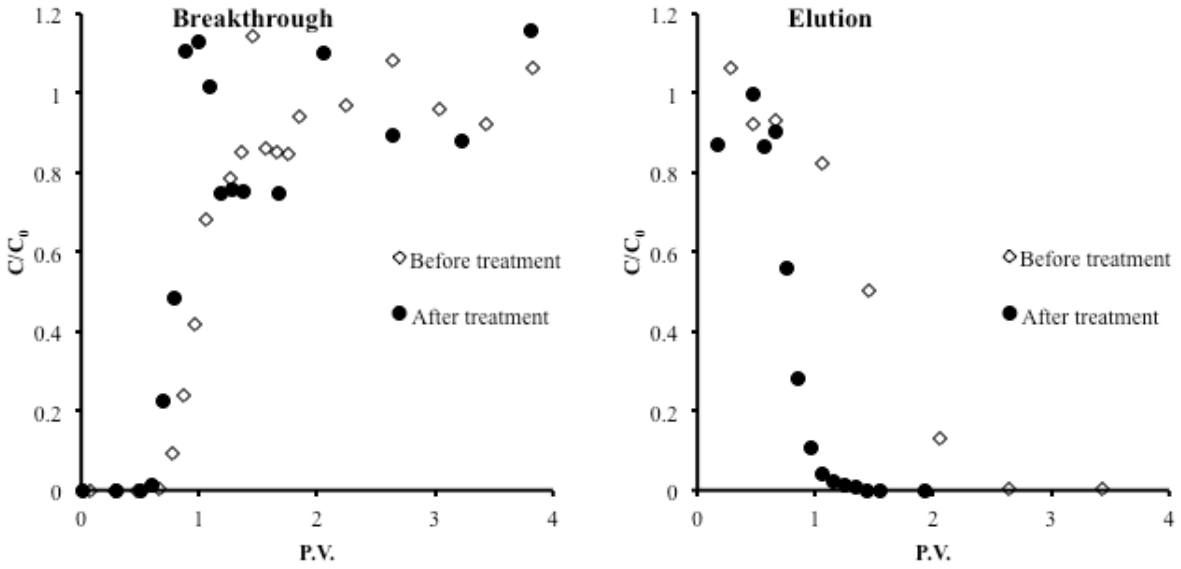

Fig. 8. Expanded view of breakthrough (Left) and elution (Right) profiles of 2,6-DFBA before and after Fe(III)-bioreduction for 20 d.

3.3 Fe(III) Bioreduction Treatment and Tracer Transport: Long-term acetate injection

Given only 0.04% of the total Fe was reduced in the short term bioreduction experiment, a second set of soil aggregate-packed column experiments (Experiment Type III) was conducted to examine the long term (59 days) effect of bioreduction on Fe(II) release and tracer transport. The experiments included replicates of acetate-stimulated Fe(III)-bioreduction columns and a control column (inoculated with *Geobacter* but not receiving acetate addition). The transport of bromide and 2,6-DFBA showed no change after the long-term bioreduction treatment, whereas SSSNP was completely retained in the soil aggregates during the tracer experiments both before and after the acetate injection (Fig.10 and Table 2). This result is inconsistent with the observation in the short term (20 days) experiments with acetate addition, where Fe(III) reduction enhanced SSSNP transport and earlier breakthrough of 2,6-DFBA.

The release of soluble Fe(II) in the long term experiment was very similar to that observed in the short term experiments during the first 20 days but exhibited a steady increase in Fe(II) concentration until reaching a plateau level around day 50 (Fig. 11). The plateau concentration of soluble Fe(II) reached 300 µM, more than 10 times that observed at the end of the short-term Fe(III) bioreduction experiment. The accumulated amount of soluble Fe(II) collected in the effluent was 80 mg or about 0.48% of the total Fe in the column. Interestingly, unlike the short-term experiment, colloids were detected in the effluent beyond 30 days of the Fe(III)-bioreduction treatment. The colloid concentrations continued to increase throughout the remainder of the acetate injection phase (Fig. 11). This result suggests the possibility of soil aggregate breakdown. A small amount of Fe(II) was also observed in the effluent of the control column indicating that *Geobacter* was able to couple oxidation of the native soil organic carbon with Fe(III) reduction.

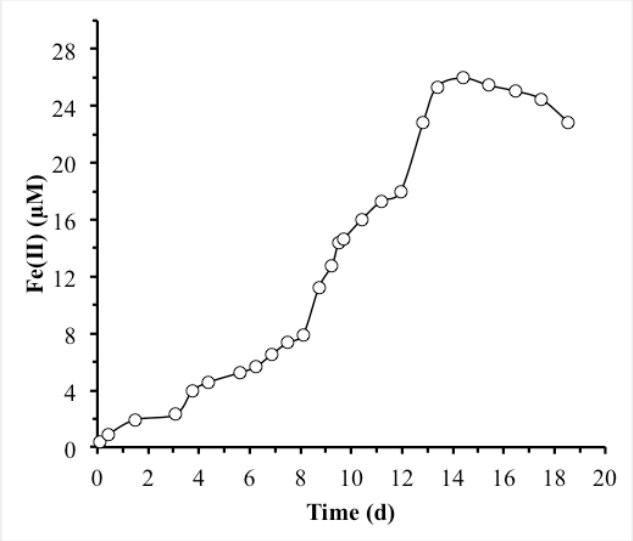

Fig. 9. Efflent Fe(II) concentration during the acetate injection (Fe(III)-bioreduction) phase of the experiment.

Table 2. Model fitted parameters for 2,6-DFBA and SSSNP breakthrough curves from water-stable soil aggregate columns before (Pre-) and after (Post-) Fe(III)-bioreduction.

Tracer	Parameter	§Fe(III)-Bioreduction phase (20 d)		Fe(III)-Bioreduction phase (60 d)					
				Column A		Column B		Column C	
		#Pre	*Post	Pre	Post	Pre	Post	Pre	Post
2,6-DFBA	D (cm)	1.12	0.93	0.89	0.84	0.85	0.82	0.84	0.83
	K_d (cm^3mg^{-1})	0.086	0.0063	0.014	0.011	0.041	0.031	0.027	0.001
	S_{max}	23.6	5.55	ϕ -	-	-	-	-	-
SSSNP	Att. Coeff. (min^{-1})	0.046	0.026	-	-	-	-	-	-
	Detach Coeff (min^{-1})	$3x10^{-6}$	$7.7x10^{-4}$	-	-	-	-	-	-

§Data were collected from a single column

#Tracer transport experiment before stimulation of Fe(III)-bioreduction by injection of acetate.

*Tracer transport experiment after Fe(III)-bioreduction by injection of acetate

ϕBreakthrough of SSSNP colloids was not detected in either the treated or control columns.

D is dispersivity

K_d is sorption coefficient

S_{max} [N_c M^{-1}] is the maximum solid phase concentration of SSSNP colloids

The contradictory results of tracer transport during the short-term and long-term Fe(III)-bioreduction experiments are difficult to reconcile. Despite more than 10 fold more Fe(III)-reduction, during the long-term experiment, there was no difference in the transport of bromide, 2,6-DFBA and SSSNP before and after the acetate injection phase. Soil aggregate breakdown might have exposed more bioavailable Fe(III) oxides existing in the interior of aggregates, resulting in fresh iron oxide surfaces, which favored the retention of SSSNP.

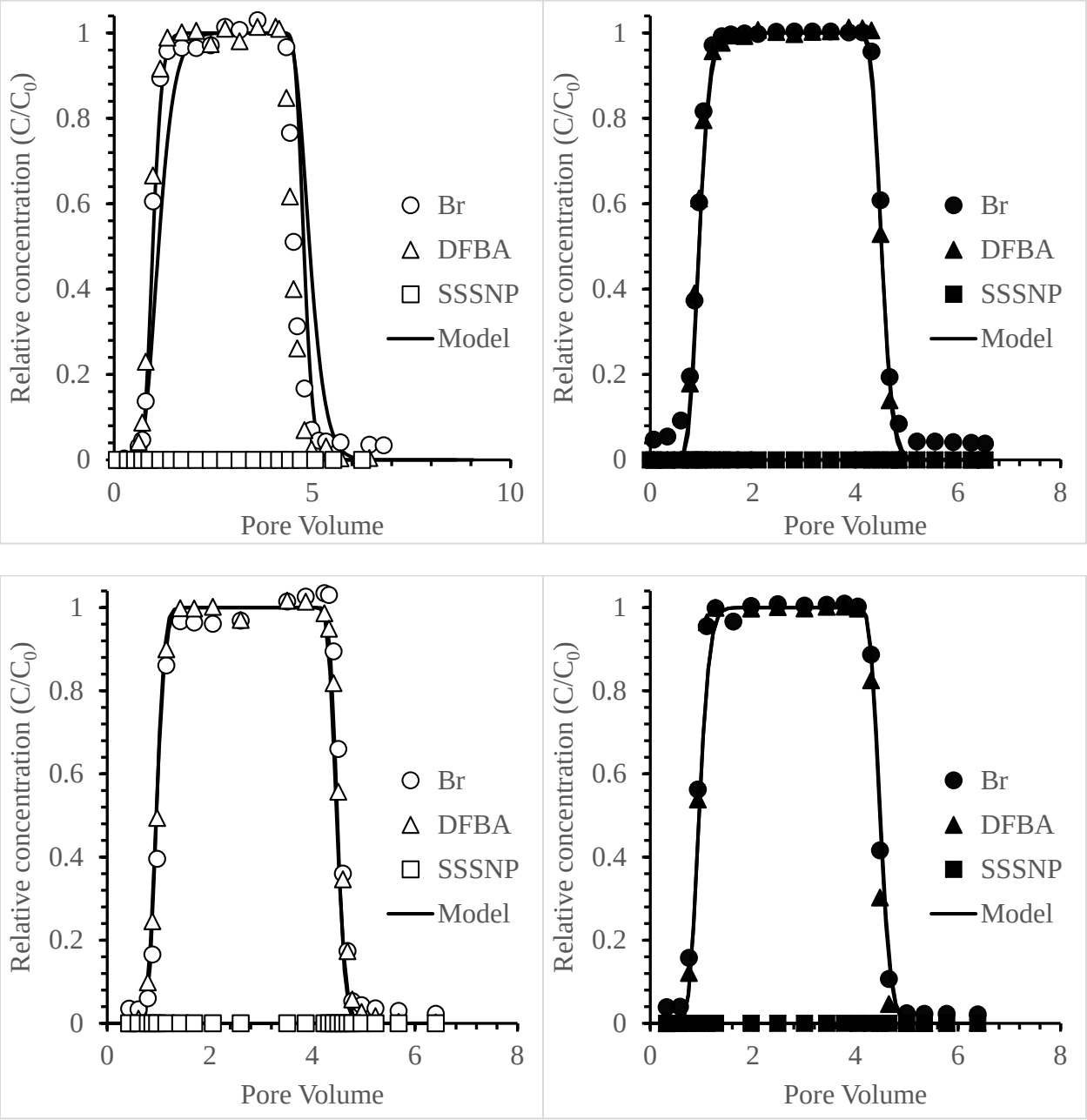

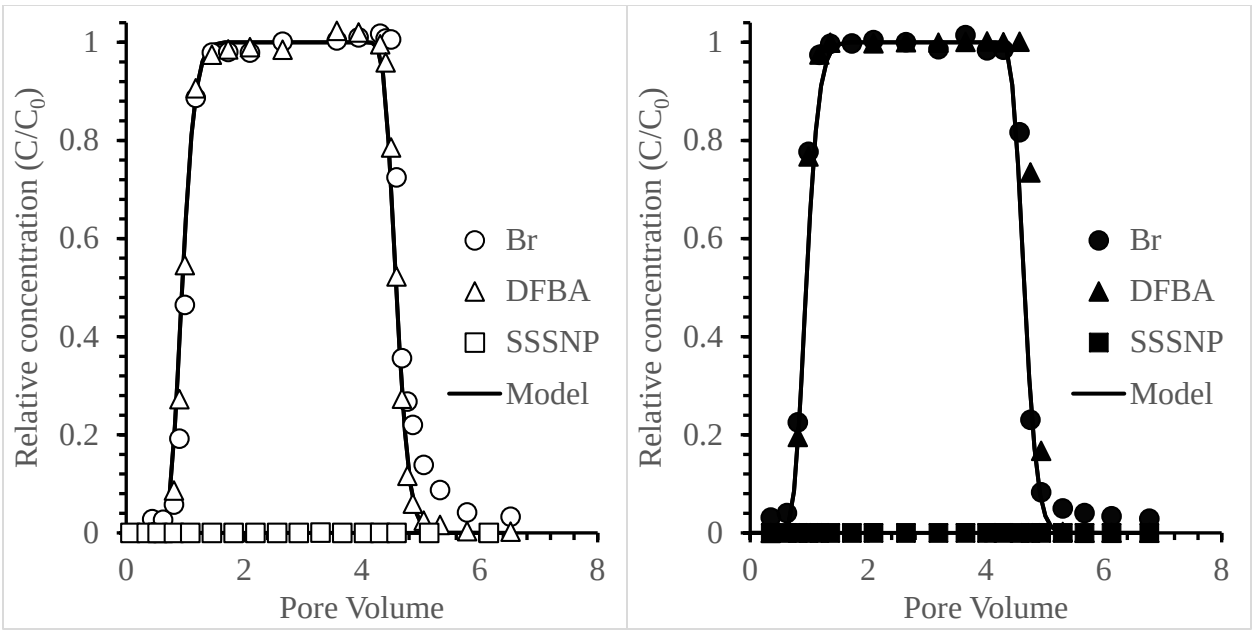

Fig. 10. BTCs of tracers in pre- (left) and post-acetate (right) treatment transport experiments for long term Fe(III)-bioreduction treatment in macroaggregates (2000-56 µm) columns. The plots on the upper and center panels are BTCs from replicate acetate-treated columns while lower two panel are BTCs from the control column that did not receive acetate injection.

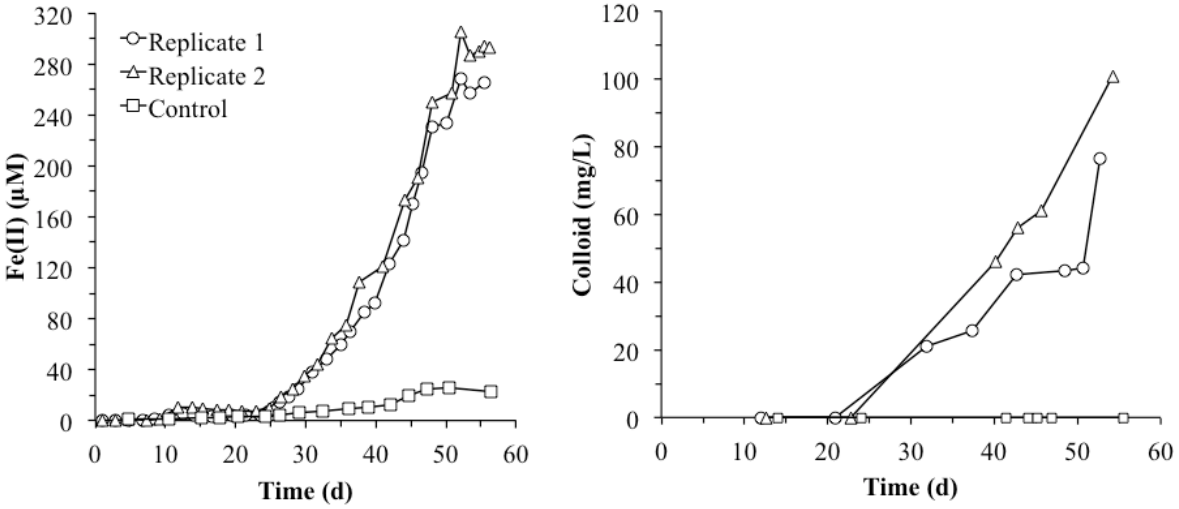

Fig. 11. Concentration of Fe(II) (left) and colloids (right) in column effluent during the acetate injection phase of the long-term Fe(III)-bioreduction experiment.

3.4 Effect of Aggregate Size Fractions on Tracer Transport

To determine if the observed transport differences of 2,6-DFBA and SSSNP between the short-term and long-term Fe(III) bioreduction experiments were the result of primarily physical changes in pore-structure or changes in chemically reactive surfaces, transport experiments were conducted in columns packed with water-stable soil aggregates of different size fractions, such as macroaggregates (250-2000 µm) and microaggregates (53-250 µm), under aerobic conditions

and without any reduction of Fe(III) oxides (Table 3). No obvious differences were observed for bromide transport between macroaggregate and microaggregate packed columns (Fig. 12). However, 2,6-DFBA was retarded in both size fractions of aggregates, with stronger retardation in the columns packed with the microaggregate size fraction (K_d of 0.12) than macroaggregates fraction(K_d of 0.057). Since the surface properties of macroaggregates and microaggregates should have been very similar, the stronger retardation may be ascribed to the greater total surface area of the microaggregates. SSSNP breakthrough was negligible in both aggregate fractions likely due to the interaction with iron oxides (Fig. 12).

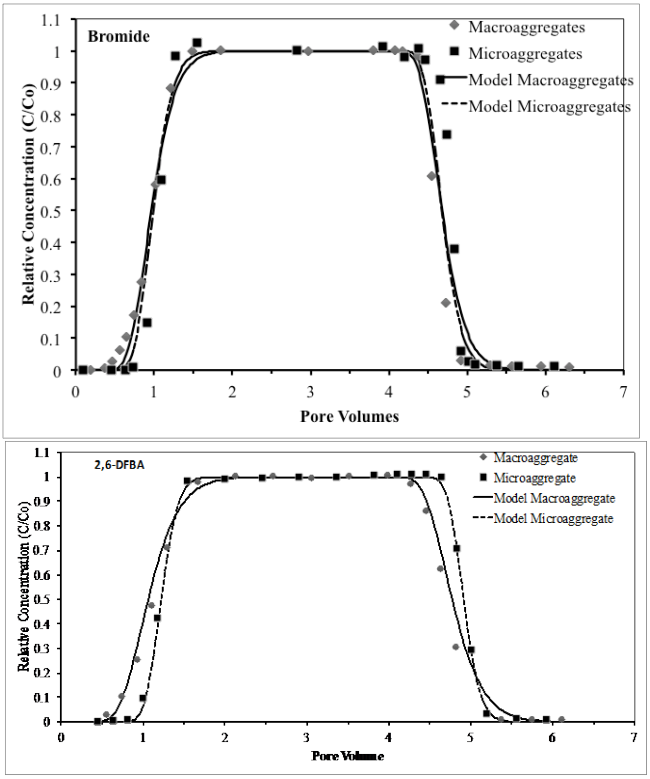

Fig. 12. Bromide and 2,6 DFBA transport in soil columns packed with water-stable macroaggregae fraction (2000-250 μm) or water-stable soil microaggregate fraction (250 -56 μm) under aerobic conditions without Fe(III)-bioreduction.

3.5. Microbial Community Structure

Principal components analysis of the sequence data revealed that the microbial community structure of the acetate-treated columns were distinct from the control column that did not receive acetate injection (Fig. 13). Within the acetate-treated columns (Columns A and B) that exhibited active Fe(III)-bioreduction, the microbial community structure varied in each of the five segments along the flow path suggesting that Fe(III)-bioreduction activity may have varied along the flow path with Segment 5 nearest the influent end and Segment 1 at the effluent end. The microbial communities in each segment of the replicated treatment columns clustered together suggesting that the communities in the acetate-treated columns were experiencing similar environmental conditions along the flow path and responded similarly to these conditions (Fig. 13). An examination of the relative abundance of various major phyla indicated that the Proteobacteria and Firmicutes had the greatest relative abundances in the treated columns especially at the influent end of the columns (Fig. 14). The high relative abundance of Proteobacteria near the influent end of the columns and the decrease along the flow path is consistent with the inoculation of the columns with *Geobacter sulfureducens* since this genus is a member of the delta-Proteobacteria. The higher relative abundance of Proteobacteria at the influent of the columns is consistent with increased growth and activity of these bacteria nearest the acetate injection site. These values decreased progressively in the soil segments toward the effluent end of the columns presumably because the acetate concentration may have become

limiting near the effluent end of the columns. The relative abundance of these two dominant phyla did not vary with distance from the influent end in the control column since the control did not receive acetate. Interestingly, the relative abundance of the group of "Unclassified Bacteria" was low at the influent end and progressively increased along the flow path reaching a maximum at the effluent end of the treated columns. In the control column this group was greatest in Segment 3 and lowest in Segments 5 and 1 (Fig. 14). Based on these data it is not possible to determine what processes or conditions that brought about changes in the relative abundance of this cryptic Phylum.

To confirm that the changes in the relative abundance of the Phylum Proteobacteria was likely due variation in the abundance and growth of *Geobacter* sp in the acetate treated columns, the sequence data was examined more closely for the relative abundance of *Geobacter* by soil segmentation. As predicted, the RA of *Geobacter* was clearly the greatest in the influent ends of the acetate-treated columns and decreased steadily in the segments near the effluent end of the columns. This is further evidence that the inoculated *Geobacter* added to the columns and/or indigenous Fe(III)-reducing bacteria were actively growing and reducing Fe(III).

3.6 Iron and colloid concentrations of extracted column sections.

The total extractable iron concentration was much higher in the inlet segments of the acetate-treated columns ranging from about 20-25 mM (Fig. 16). The total iron concentration in the soil segments near the effluent end of the treated columns was less than 5 mM. In the control column that did not receive acetate injection, the total iron concentration was 4.5-5.5 mM and less than 1mM in the influent and effluent ends of the column, respectively. A similar trend was observed for the extractable colloid concentration (Fig. 16; upper panel). In the influent segment of the treated columns, the colloid concentration was 12.5 mg ml^{-1} while the effluent end segments released only 2.5 mg ml^{-1}. These trends were very similar to the distribution of *Geobacter sp.* in the columns suggesting that Fe(III)-bioreduction by *Geobacter sp.* contributed to iron and colloid release.

Conclusions and Implications for Future Research/Implementation

Colloid Generation/Pore Accessibility: The microbially mediated Fe(III)-oxide reduction was demonstrated to have significant effect on the transport of molecular and colloidal tracers (but not on the ionic tracer Br^-) and colloid generation depending on the duration of the bioreduction process. In the short-term bioreduction experiment tracer transport was enhanced after Fe(III)-bioreduction while in the long-term bioreduction experiment there was no difference in tracer transport before and after Fe(III)-bioreduction despite considerably more Fe(II) and colloid released in the column effluent. These results are difficult to reconcile without additional research. Our current working hypothesis is that in the short duration Fe(III)-bioreduction experiment, only Fe(III)-oxides coating the exterior surfaces of soil aggregates were reduced yielding advective flow paths with chemically less reactive surfaces allowing enhanced tracer (2,6-DFBA and SSSNP) transport with only minimal aggregate dispersion. Considerably more aggregate dispersion was observed in the long-term bioreduction experiment suggesting perhaps that new Fe(III)-oxide surfaces may have become exposed yielding more reactive surface area and tracer breakthrough curves similar to those observed before Fe(III)-bioreduction. It is impossible to confirm this hypothsis with the data presented in this report. Further chemical

characterization of the solid phase porous media would be needed to address this speculation. A physical analysis of a change in the distribution of aggregate size fractions was inconclusive (data not shown).

Bioreduction/Re-oxidation. Electron-donor addition during biostimulation cannot continue indefinitely. Thus upon termination of biostimulation, the treated area will ultimately return to its original redox status as oxygenated groundwater passes through the treatment zone. There is some uncertainty regarding how a return to a higher redox potential may affect chemical and hydrologic properties of the porous media. In the work reported here, time and resources were insufficient to complete experiments addressing re-oxidation or the influence of down-gradient redox changes on the chemical, physical, and biological properties of the porous media. Future studies should investigate potential changes in the hydraulic properties of packed columns containing subsurface porous media in a similar fashion as described above but include re-oxidation phase as an additional treatment (see Figure 17; control column not pictured). The same effluent and pressure measurements as described should be performed during the experiment. At the conclusion of the proposed experiments, the columns should be deconstructed and pore water and solid phase analyses to examine changes in Fe mineralogy along the flow path completed. Additionally, advanced imaging analyses such as those proposed by Dr. Jardine in the original proposal could be attempted to assess changes in pore-structure as the result of Fe(III)-bioreduction. Finally, to address secondary impacts to water quality down-gradient of the bioreduction zone, a similar experimental system using reduced and oxidized columns connected in series could be employed to simulate

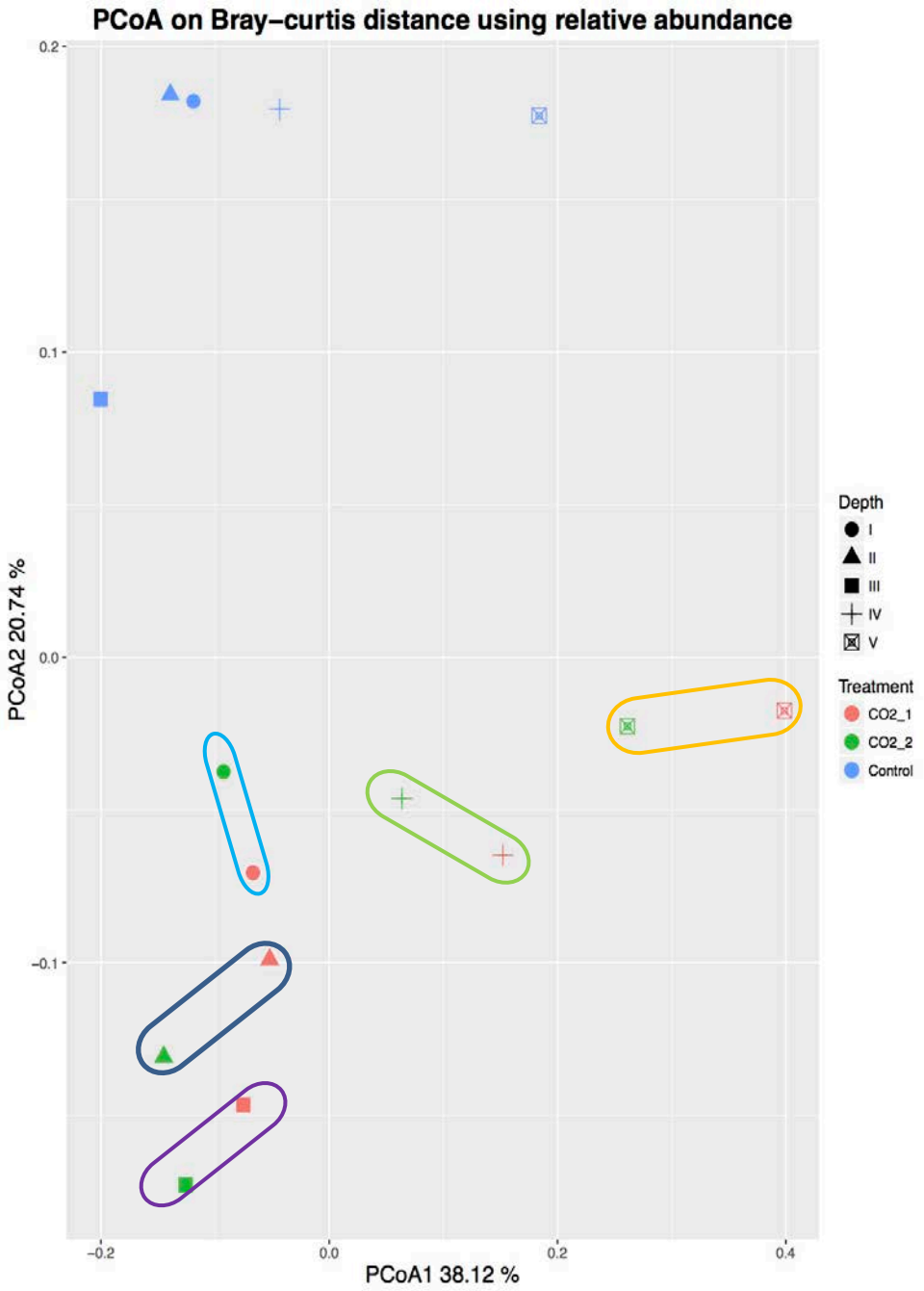

Fig. 13. Principal components analysis of bacterial relative abundance at the phylum level in replicate acetate treated columns and the control column that did not receive acetate injection. Soil in the columns was sectioned into five sections along the flow path with section 5 nearest the influent end and section 1 at the effluent end.

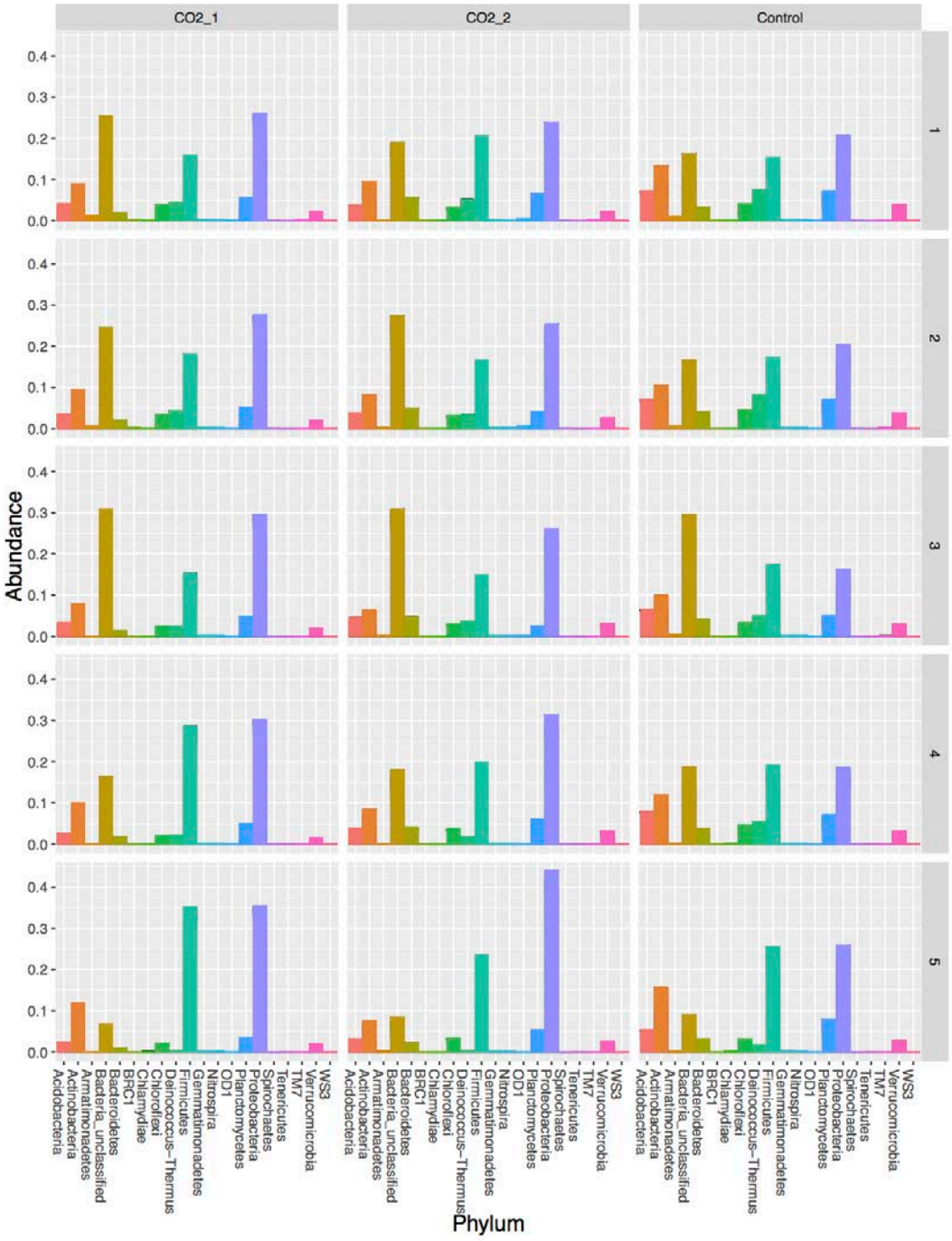

Fig. 14. Relative abundance of major bacterial phyla in the acetate-treated columns that exhibit Fe(III)-bioreduction (replicate columns 1 and 2) and control column that did not receive acetate. At the conclusion of the post-treatment tracer test, columns were divided into five sections along the flow path with section 5 nearest the influent end and section 1 at the effluent end.

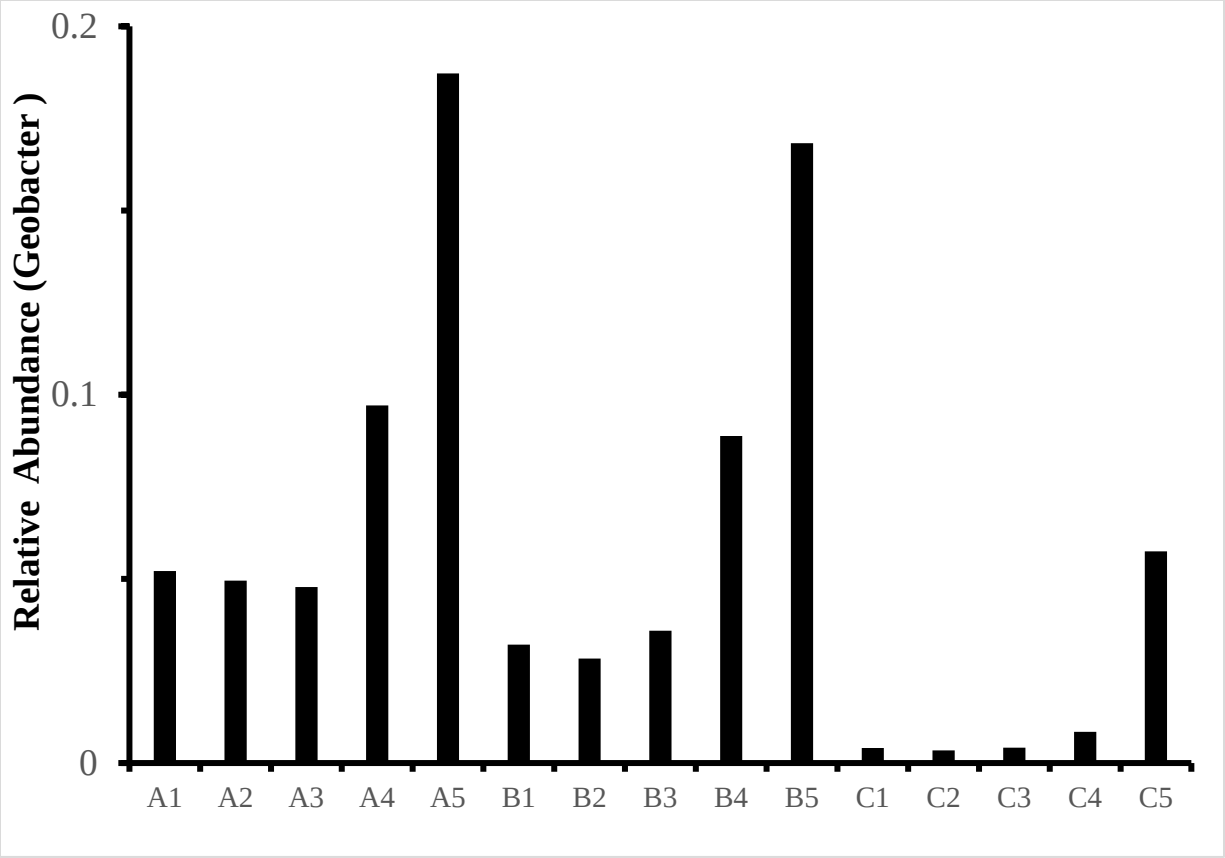

Fig. 15. Relative abundance of *Geobacter* sp. in acetate amended (A1-5 and B1-5) and control (C1-5) columns containing water-stable soil aggregates (2000-56 □m). The numbers refer to sections of the column along the flow path with section 1 nearest the effluent end and section 5 nearest the influent end.

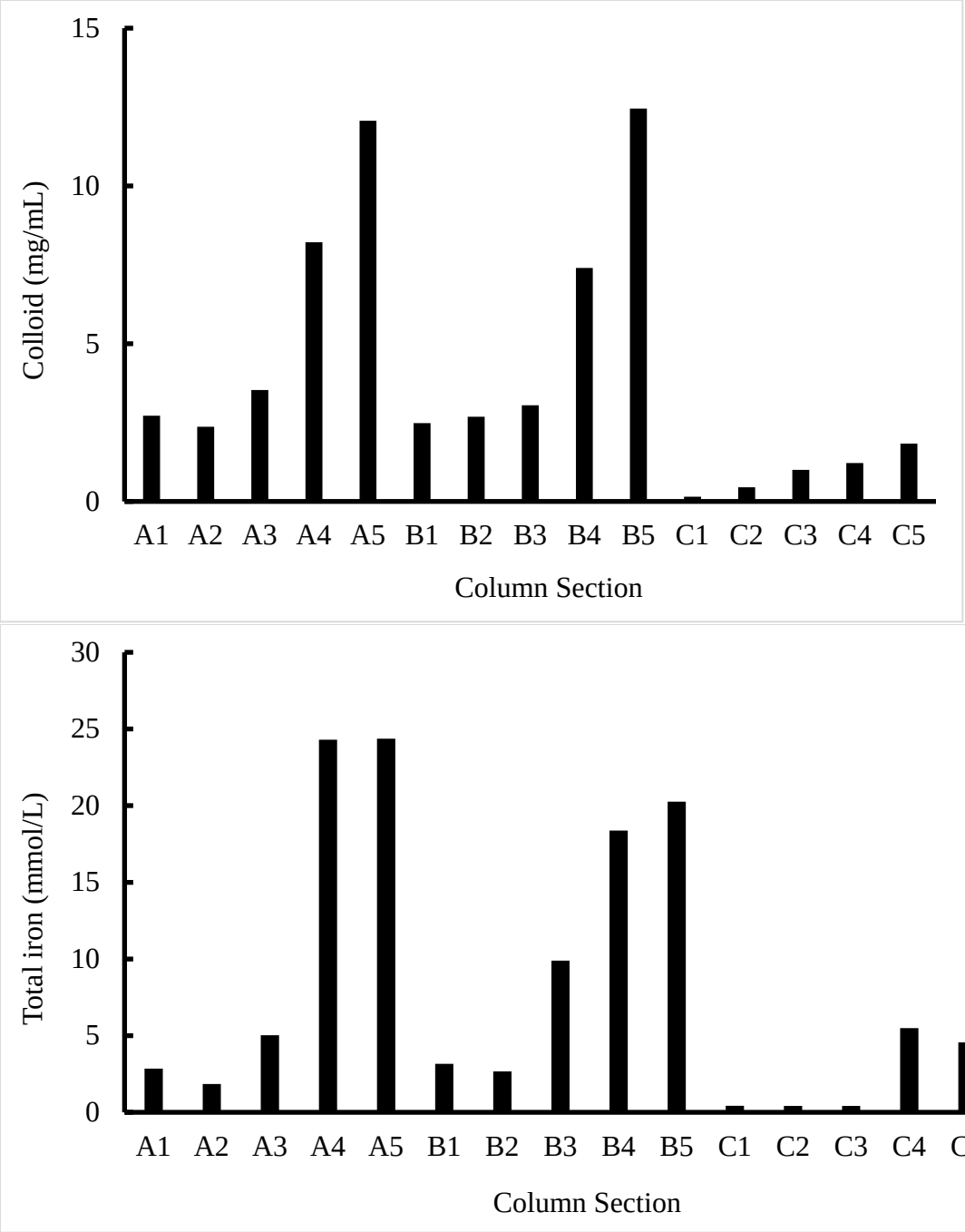

Fig. 16. Phosphate-extractractable colloid (upper panel) and iron (lower panel) concentrations of the sectioned columns at the conclusion of the long-tern Fe(III) bioreduction experiment. Columns A and B were treated with acetate for 60 d and column C, the control column, did not receive any acetate. Section 1 and 5 represent the effluent and influent ends of the columns, respectively.

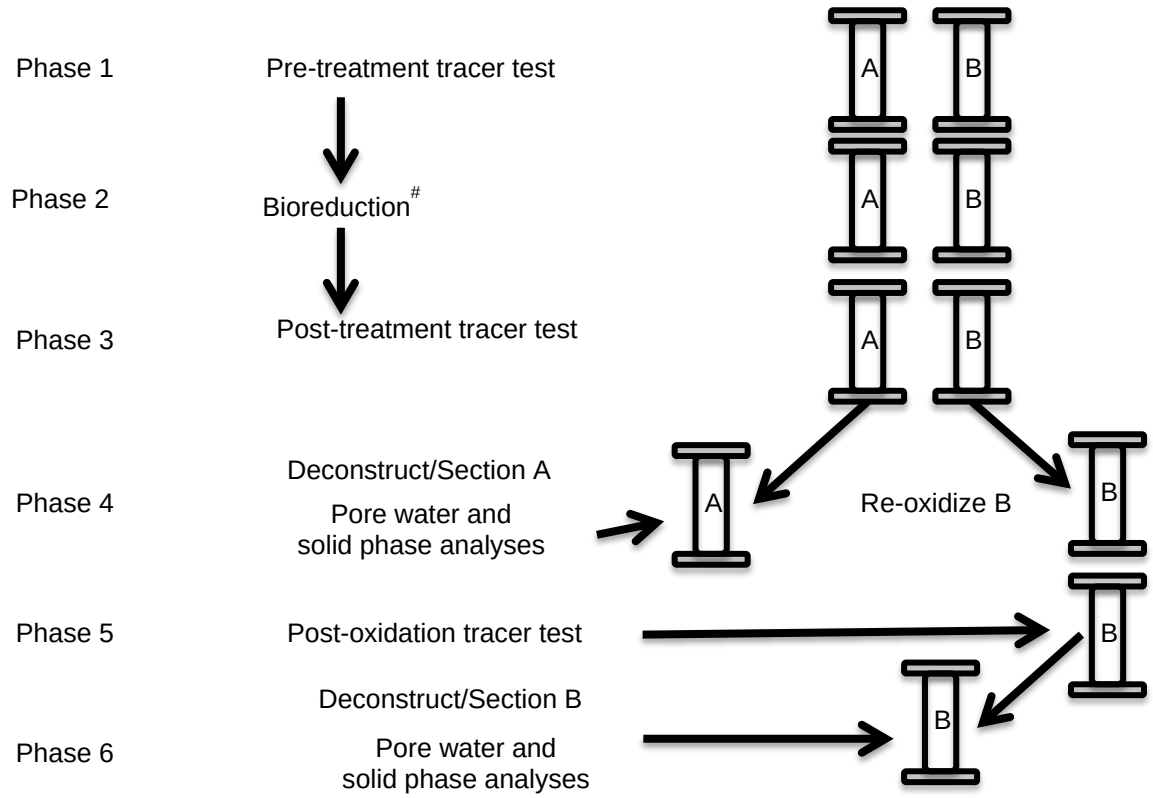

Fig. 17. Diagram showing the execution of a six-phase bioreduction experiment with a re-oxidation phase included as an additional treatment.

Literature Cited

1. Aulenta, F., M. Majone, and V. Tandoi. 2006. Enhanced anaerobic bioremediation of chlorinated solvents: environmental factors influencing microbial activity and their relevance under field conditions. **Chemical Technology and Biotechnology** 81(9), 1463-1474.
2. Bose, P., and A. Sharma. 2002. Role of iron in controlling speciation and mobilization of arsenic in subsurface environment. **Water Research** 36(19), 4916–4926. DOI: 10.1016/S0043-1354(02)00203-8
3. Bradford, S.A. and S. Torkzaban. 2008. Colloid transport and retention in unsaturated porous media: a review of interface-, collector-, and pore-scale processes and models. **Vadose Zone Journal** 7(2), 667-681. DOI:10.2136/vzj2007.0092
4. Caccavo, F., D.J. Lonergan, D.R. Lovley, M. Davis, J.F. Stolz, and M.J. McInerney. 1994. Geobacter sulfurreducens sp. Nov., a hydrogen- and acetate-oxidizing dissimilatory metal-reducing microorganism. **Applied and Environmental Microbiology** 60(10), 3752-3759.
5. Caldwell, M.E., R.S Tanner, and J.M Suflita. 1999. Microbial metabolism of benzene and the oxidation of ferrous iron under anaerobic conditions: implications for bioremediation. **Environmental Microbiology** 5(6), 595-565. DOI: 10.1006/anae.1999.0193
6. Chapelle, F.H., and D.R. Lovley. 1992. Competitive exclusion of sulfate reduction by fe(lll)-reducing bacteria: a mechanism for producing discrete zones of high-iron ground water. **Ground Water**. DOI: 10.1111/j.1745-6584.1992.tb00808.
7. Coates, J.D., and R.T. Anderson. 2000. Emerging techniques for anaerobic bioremediation of contaminated environments. **Trends in Biotechnology** 18(10), 408-412. DOI: 10.1016/S0167-7799(00)01478-5
8. De-Camposa, A., A.I. Mamedovb, and C-I. Huang. 2009. Short-term reducing conditions decrease soil aggregation. **Soil Science Society of America Journal** 73, 550-559
9. Ellis, D.E., E.J. Lutz, J.M. Odom, R.J. Buchanan, C.L. Bartlett, M.D. Lee, M.R. Harkness, and K.A. DeWeerd. 2000. Bioaugmentation for accelerated in situ anaerobic bioremediation. **Environmental Science and Technology** 34 (11), 2254–2260. DOI: 10.1021/es990638e
10. Goldberg, S., and R.A. Glaubig. 1987. Effect of saturating cation, pH, and aluminum and iron oxide on the flocculation of kaolinite and montmorillonite. **Clays and Clay Minerals** 35, 220-227.
11. Goldberg, S., B.S. Kapoor, and J.D. Rhoades. 1990. Effect of aluminum and iron oxides and organic matter on flocculation and dispersion of arid zone soils. **Soil Science** 150(3), 588-593.
12. Hansel, C.M., S.G. Benner, J. Neiss, A. Dohnalkova, R.K Kukkadapu, and S. Fendorf. 2003. Secondary mineralization pathways induced by dissimilatory iron reduction of ferrihydrite under advective flow. **Geochimica et Cosmochimica Acta** 67(16), 2977–2992. DOI: 10.1016/S0016-7037(03)00276-X
13. Hansel, C.M., S.G. Benner, and S. Fendorf. 2005. Competing Fe(II)-induced mineralization pathways of ferrihydrite. **Environmental Science and Technology** 39, 7147-7153.

14. Hassellov, M., and F. von der Kammer. 2008. Iron oxides as geochemical nanovectors for metal transport in soil-river systems. **Elements** 4, 401-406.

15. Kozich, J.J., S.L. Westcott, N.T. Baxter, S.K. Highlander, and P.D. Schloss. 2013. Development of a dual-index sequencing strategy and curation pipeline for analyzing amplicon sequence data on the MiSeq Illumina sequencing platform. **Applied and Environmental Microbiology** 79(17), 5112-5120.

16. Kubica, P., H. Garraud, J. Szpunar, and R. Lobinski. 2015. Sensitive simultaneous determination of 19 fluorobenzoic acids in saline waters by solid-phase extraction and liquid chromatography–tandem mass spectrometry. **Journal of Chromatography A** 1417, 30-40. DOI: 10.1016/j.chroma.2015.09.024

17. Kuhnen, F., K. Barmettler, S. Bhattacharjee, M. Elimelech, and R. Kretzschmar. 2000. Transport of iron oxide colloids in packed quartz sand media: monolayer and multilayer deposition. **Journal of Colloid and Interface Science** 231(1), 32-41. DOI: 10.1006/jcis.2000.7097

18. Jardine, P.M. 2008. Influence of coupled processes on contaminant fate and transport in subsurface environment. (ed.) D.L. Sparks. **Advances in Agronomy** 99, 1-99.

19. Maurice, P.A., and M.F. Hochella. 2008. Nanoscale particles and processes: a new dimension in soil science. 100th Anniversary edition, **Advances in Agronomy** 100, 123-153.

20. Mayes, M.A., P.M. Jardine, T.L. Mehlhorn, B.N. Bjornstad, J.L. Ladd, and J.M. Zachara. 2003. Hydrologic processes controlling the transport of contaminants in humid region structured soils and semi-arid laminated sediments. **Journal of Hydrology** 275, 141-161.

21. McCarthy, J.F., and L.D. McKay. 2004. Colloid transport in the subsurface: past, present and future challenges. **Vadose Zone Journal** 3(2), 326-337. DOI:10.2136/vzj2004.0326

22. McKay, L.D., W.E. Sanford, and J.M. Strong. 2000. Field-scale migration of colloidal tracers in a fractured shale saprolite. **Ground Water** 38(1), 139-147. DOI: 10.1111/j.1745-6584.2000.tb00211.x

23. Methé, B.A., K.E. Nelson, J.A. Eisen, I.T. Paulsen, W. Nelson, J.F. Heidelberg, D. Wu, M. Wu, N. Ward, M.J. Beanan, R.J. Dodson, R. Madupu, L.M. Brinkac, S.C. Daugherty, R.T. DeBoy, A.S. Durkin, M. Gwinn, J.F. Kolonay, S.A. Sullivan, D.H. Haft, J. Selengut, T.M. Davidsen, N. Zafar, O. White, B. Tran, C. Romero, H.A Forberger, J. Weidman, H. Khouri, T.V. Feldblyum, T.R. Utterback, S.E. Van Aken, D.R. Lovley, and C.M. Fraser. 2003. Genome of geobacter sulfurreducens: metal reduction in subsurface environments. **Science** 302, 5652, 1967-1969. DOI: 10.1126/science.1088727

24. Pedersen, H.D., D. Postma, and R. Jakobsen. 2006. Release of arsenic associated with the reduction and transformation of iron oxides. **Geochimica et Cosmochimica Acta** 70(16), 4116–4129. DOI: 10.1016/j.gca.2006.06.1370

25. Stookey, LL. 1970. Ferrozine—a new spectrophotometric reagent for iron. **Analytical Chemistry** 42(7), 779-781.

26. Thompson, A., O.A. Chadwick, S. Boman, and J. Chorover. 2006. Colloid mobilization during soil iron redox oscillations. **Environmental Science and Technology** 40 (18), 5743–5749. DOI: 10.1021/es061203b

27. Vilks, P., L.H. Frost, and D.B. Bachinski. 1997. Field-scale colloid migration experiments in a granite fracture. **Journal of Contaminant Hydrology** 26(1–4), 203-214. DOI: 10.1016/S0169-7722(96)00069-1

28. Viollier, E., P.W. Inglett, K. Hunter, A.N. Roychoudhury, and P. van Cappellen. 2000. The ferrozine method revisited: Fe(II)/Fe(III) determination in natural waters. **Applied Geochemistry** 15(6), 785-790.

29. Weber, K.A., L.A. Achenbach, and J.D. Coates. 2006. Microorganisms pumping iron: anaerobic microbial iron oxidation and reduction. **Nature Reviews Microbiology** 4, 752-764. DOI: 10.1038/nrmicro1490

30. Yan, J., K.M. Ritalahti, D.D. Wagner, and F.E. Loffler. 2012. Unexpected specificity of interspecies cobamide transfer from Geobacter spp. To organohalide-respiring Dehalococcoides mccartyi strains. **Applied and Environmental Microbiology** 78(18), 6630-6636.

31. Zhuang, J., Y. Jin, and M. Flury. 2003. Colloid-facilitated cesium transport through water-saturated Hanford sediment and Ottawa sand. **Environmental Science and Technology**, 37(21), 4905-4911. DOI: 10.1021/es0264504

32. Zhuang, J., M. Flury, and Y. Jin. 2004. Comparison of Hanford colloid and kaolinite transport in porous media. **Vadose Zone Journal** 3(2), 395-402.

33. Zhuang, J., J. Qi, and Y. Jin. 2005. Retention and transport of amphiphilic colloids under unsaturated flow conditions: effect of particle size and surface properties. **Environmental Science and Technology** 39(20), 7853-7859. DOI: 10.1021/es050265j.

34. Zhuang, J., J.F. McCarthy, E. Perfect, J. Tyner, M. Flury, and T. Steenhuis. 2007. In-situ colloid mobilization in Hanford sediments under unsaturated transient flow condition: Effect of irrigation pattern. **Environmental Science and Technology** 41(9), 3199-3204. DOI: 10.1021/es062757h.

35. Zhuang, J., and Yan Jin. 2008. Interactions between virus and goethite during saturated flow: effects of solution pH, carbonate, and phosphate. **Journal of Contaminant Hydrology** 98(1-2), 15-21. DOI: 10.1016/j.jconhyd.2008.02.002.

36. Zhuang, J., J.S. Tyner, and E. Perfect. 2009. Colloid transport and remobilization in unsaturated porous media during transient flow. **Journal of Hydrology** 377, 112-119. DOI: 10.1016/j.jhydrol.2009.08.011

Appendicies of Supporting Data

Transport of SSSNP in Clean Quartz Sand

Date	1/14/16	
Media	Clean fine sand	
	Column 1	Column 2
Mass of packing (g)	467.6	463
Volume of Column (ml)	286	286
Pore Volume (ml)	109.5	111.3
Dead Volume (ml)	8	8
Pump tubing (I.D. mm)	0.89	0.89
Pump speed (rpm)	25.5	25.5
Flow rate (ml/min.)	1.8	1.82
Darcy flux (cm/min)	0.158	0.159
Pore velocity (cm/min.)	0.412	0.410
Fraction collection (min/tube)	8	8

Tracer concentration:	40 ppb SSNP
Eluting solution:	50 ppm (0.67 mM) KCl
Tracer time(min)	232

Transport of SSSNP in Goethite-coated sand

Date:	1/25/16	
Media	Goethite-coated sand	
	Column 1	Column 2
Mass of packing (g)	460.7	466.8
Volume of Column (ml)	286	286
Pore Volume (ml)	112.15	109.8
Dead Volume (ml)	8	8
Pump tubing (I.D. mm)	0.89	0.89
Pump speed (rpm)	25.5	25.5
Flow rate (ml/min.)	1.8	1.8
Darcy flux (cm/min)	0.158	0.158
Pore velocity (cm/min.)	0.404	0.411
Fraction collection (min/tube)	8	8

Tracer concentration:	40 ppb SSNP
Eluting solution:	50 ppm (0.67 mM) KCl
Tracer time(min)	240

Short-term Fe(III) Bioreduction in Water Stable Soil Aggregates

Date: 4/7/16
Media: Soil aggregates (250-2000 μm)

	Pre-treatment Tracer	Post-treatment Tracer
Mass of packing (g)	296	296
Volume of Column (ml)	286	286
Pore Volume (ml)	174.3	174.3
Dead Volume (ml)	12.1	12.1
Pump tubing (I.D. mm)	0.89	0.89
Pump speed (rpm)	25	25
Flow rate (ml/min.)	1.7	1.69
Darcy flux (cm/min)	0.15	1.48
Pore velocity (cm/min.)	0.246	0.243
Fraction collection (min/tube)	10	10
Tracer Solution	SSSNP, KBr, 2,6-DFBA	
Eluting solution	KCl	
Tracer vol. (ml)	615.35	1714.9
Tracer time (min)	360	1013.27

Stage 1 = Pre-treatment tracer solution
Stage 2 = Elution with KCl
Stage 3 = 1:1 diluted growth media (Acetate injection for Fe(III)-Bioreduction
Stage 4 = KCl
Stage 5 = Post-treatment tracer solution
Stage 6 = Elution with KCl

Tracer input solution = 1mM KBr; 100 μg/L 100nm SSSNP; 50 mg/L 2,6-DFBA

Long-Term Fe(III)-Bioreduction Experiment in Soil Aggregates with Artificial Groundwater

Date	7/13/16		
Media	Soil aggregates (250-2000 μm)		
	Column 1	Column 2	Control Column
Mass of packing (g)	292.4	295.5	291.3
Volume of Column (ml)	290	290	290
Pore Volume (ml)	179.6	178.5	180.07
Dead Volume (ml)	12.1	12.1	11.8
Pump tubing (I.D. mm)	0.65	0.65	0.65
Pump speed (rpm)	50	50	50
Flow rate (ml/min.)	2.04	2.02	2.07
Darcy flux (cm/min)	0.179	0.177	0.181
Pore velocity (cm/min.)	0.289	0.286	0.295
Fraction collection (min/tube)	8	8	8
Tracer vol (ml)			
Tracer time (min)	304	304	304

List of Scientific Publications

C.M. Hansel, C.L. Lentini, Y. Tang, D.T. Johnston, and S.D. Wankel, and P.M. Jardine. 2015. *Dominance of Sulfur-fueled Iron Oxide Reduction in Low Sulfate Freshwater Sediments.* ISME J. 9:2400-2412.

Y. Wang, X. Liang, J. Zhuang, M. Radosevich, and F. Löffler. 2017. *Iron Oxide Bioreduction Results in Colloid Dispersion and Aggregate Breakdown but Has Minimal Impact On Tracer Transport Through Soil.* Sci. Tot. Env. *In preparation.*

Presentations

Jardine, P.M., C.M. Hansel-Wankel, J.C. Parker, R.W. Gentry; K.G. Scheckel, U. Kim, Y. Tang, M. Stewart, and L. Le. 2011. *Assessing the Potential Consequences of Subsurface Bioremediation: Fe-oxide Bioreductive Processes and the Propensity for Secondary Mineral Precipitation, Media Structural Breakdown, and Contaminant–Colloid Co-Transport*. Annual SERDP / ESTCP workshop. Nov. 29- Dec. 1, 2011. Washington DC.

Y. Wang, X. Liang, J. Zhuang, M. Radosevich. 2016. *Impact of Anaerobic Bioremediation on Soil Structure, Colloid Formation, and Contaminant Transport.* Soil Science Society of America.

Y. Wang, X. Liang, J. Zhuang, M. Radosevich. 2016. *Impact of Anaerobic Bioremediation on Soil Structure, Colloid Formation, and Contaminant Transport.* American Geophysical Union, San Francisco, CA